This document was prepared in conjunction with work accomplished under Contract No. DE-AC09-96SR18500 with the U.S. Department of Energy.

2008 ASME Fluids Engineering Division Summer Conference
August 10 - 14, 2008, Jacksonville, Florida

FEDSM2008-55013

Experimental Bubble Formation in a Large Scale System for Newtonian and Non-Newtonian Fluids

Robert A. Leishear
Savannah River National Laboratory
Aiken, South Carolina, 29803
803-725-2832, Robert.Leishear@SRS.gov

Michael L. Restivo
Savannah River National Laboratory
Aiken, South Carolina, 29803
803-725-3355, Michael.Restivo@SRS.gov

Jeanne K. Bernards
Hanford Waste Treatment & Immobilization Plant Project
2435 Stevents Center Place
Richland, WA 99354

David J.Sherwood
Hanford Waste Treatment & Immobilization Plant Project
2435 Stevents Center Place
Richland, WA 99354

ABSTRACT

The complexities of bubble formation in liquids increase as the system size increases, and a photographic study is presented here to provide some insight into the dynamics of bubble formation for large systems. Air was injected at the bottom of a 28 feet tall by 30 inch diameter column. Different fluids were subjected to different air flow rates at different fluid depths. The fluids were water and non-Newtonian, Bingham plastic fluids, which have yield stresses requiring an applied force to initiate movement, or shearing, of the fluid. Tests showed that bubble formation was significantly different in the two types of fluids. In water, a field of bubbles was formed, which consisted of numerous, distributed, ¼ to 3/8 inch diameter bubbles. In the Bingham fluid, large bubbles of 6 to 12 inches in diameter were formed, which depended on the air flow rate. This paper provides comprehensive photographic results related to bubble formation in these fluids.

KEYWORDS

Bubbles, superficial velocity, Bingham fluid, Newtonian fluid.

INTRODUCTION

Two different sets of tests were performed to investigate bubble formation in Newtonian and non-Newtonian fluids. For one set (Guerreo, et. al. [1]), the fluids were water and AZ101 simulant, which is an opaque, Bingham plastic fluid described below. For the other set, the fluid was Laponite, which is a clear Bingham plastic fluid (Restivo, et. al. [2]). An extensive body of literature is available with respect to bubble formation. A dated survey of the literature is available from Clift, et. al. [3], describing the theory of bubble formation in small scale, bench top, systems. At present, similar theory is unavailable for large scale systems, such as the thirty feet tall system considered here. This paper presents only experimental data to provide some insight into the effects of yield stress and viscosity, or consistency, on bubble formation. An equipment description is required to understand the test data.

Equipment Description and Material Properties

Tests were performed in one of two vertical, open top columns. The variants in test conditions were the height of fluid in the columns, the type of fluid in the columns, and the superficial velocity of the air introduced at the bottom of the columns., where the superficial velocity equals the volumetric flow rate divided by the cross sectional area of the liquid surface.

The column design for the water and AZ101 tests is shown in Figs. 3 - 5, and the column for the Laponite tests is shown in Figs. 6 and 7. The primary difference between the equipment is the construction material, which was stainless steel for the water and AZ101 tests and transparent acrylic for the Laponite tests. The difference in column material necessitated the use of view ports in the stainless steel column. The axisymmetric air sparging, or supply, tube in the column was the same for both columns.

Fluid properties are listed in Table 1, and a comparison of Newtonian to Bingham fluids is shown in Fig. 1. The transparent

quality of water and the translucent quality of Laponite provide better visualization of bubbles in solution, but bubbles at the surface of the opaque AZ101 solution also provide some insight into bubble formation. By dilution, two different samples, or batches, of the AZ101 simulant were obtained for testing. The AZ101 solution is a mixture of chemicals used to simulate nuclear waste. Laponite is a commercially available synthetic silicate product.

To obtain rheological properties, a Haake RS600 rheometer was used in conjunction with a Searle Z41 sensor system. Typical data is displayed in Fig. 2, where the "up" curve is obtained while the rheometer speed is increased, and the "down' curve is obtained while the speed is decreased. To obtain the values listed in Table 1. Three separate tests are performed for each material sample, and then the first 50 data points are deleted to linearize the test results. From the linearization three yield stresses and consistencies can then be calculated and averaged to obtain the approximate material properties.

Fluid	Yield Stress Pascals	Consistency / viscosity Centipoise
Water	0	1
Laponite	132	---
AZ101	13	11.5
AZ101	30	27.7

Table 1: Fluid Properties

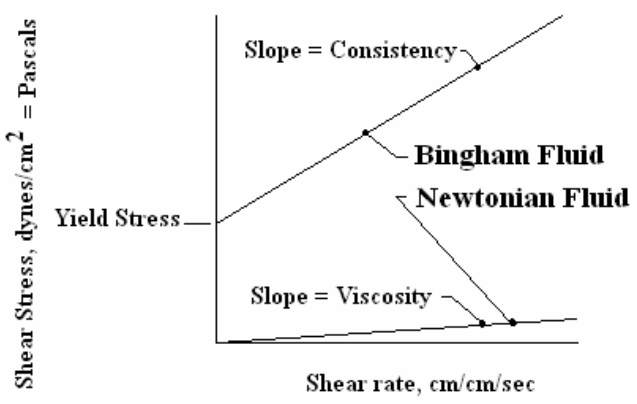

Figure 1: Fluid Characteristics

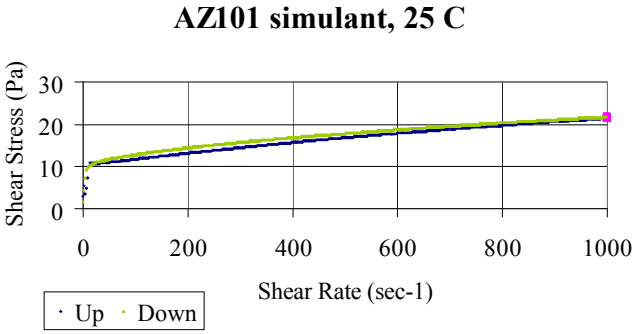

Figure 2: Typical Test Results for Rheological Properties

Figure 3: Column Installation for Water and AZ101 Testing

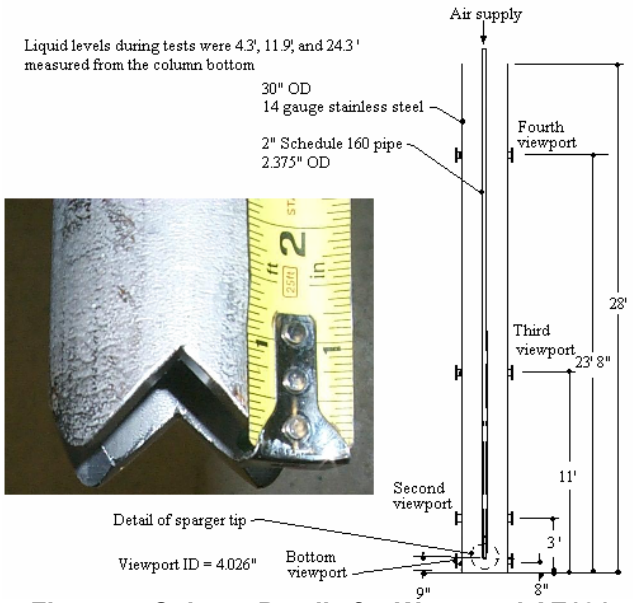

Figure 4: Column Details for Water and AZ101 Testing

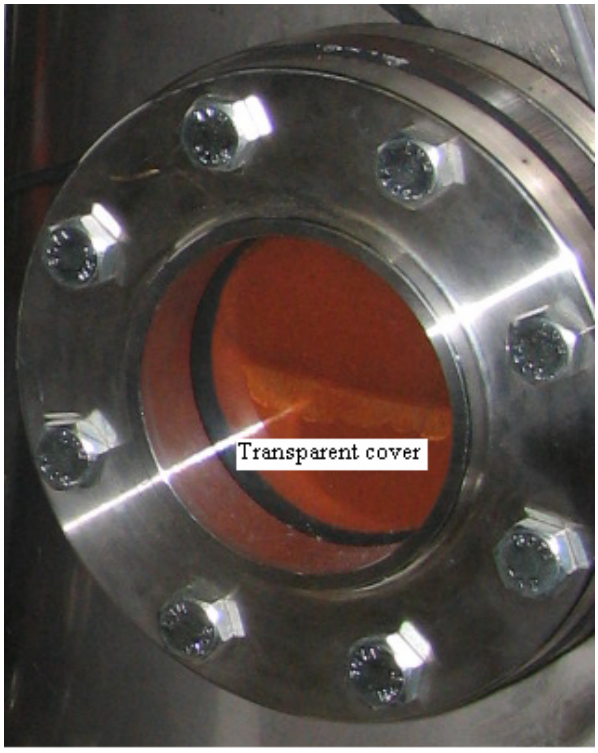

Figure 5: Viewport Detail, AZ101 shown

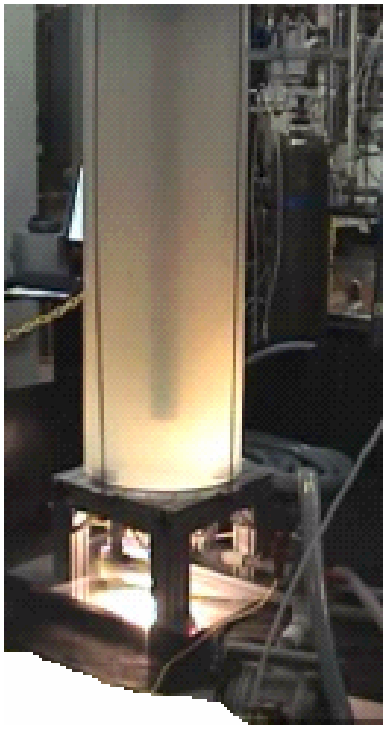

Figure 6: Column Installation for Laponite Testing

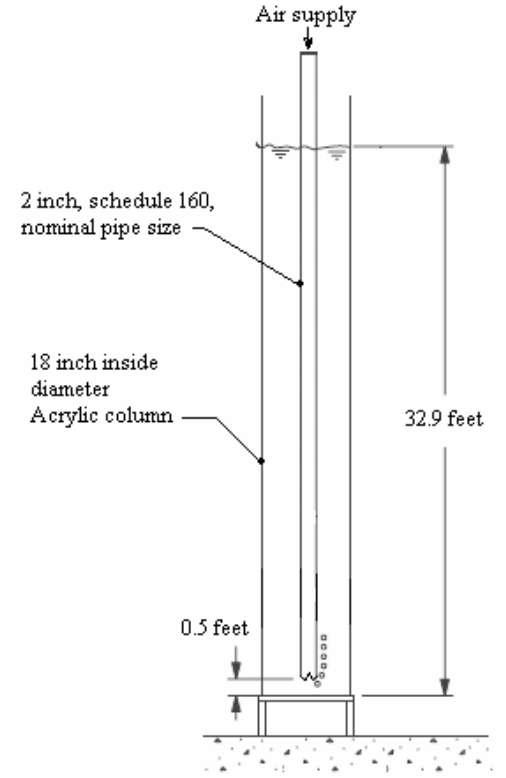

Figure 7: Column Details for Laponite Testing

RESULTS

A definition of flow regimes assists the description of bubble formations (Shaikh and Al-Dahlan [4]). As the localized air flow rate increases, bubble characteristics change. At low flows, cylindrical Stoke's bubbles are formed. As the flow increases, the bubbles become hemispherical Taylor bubbles. Finally the flow becomes churn-turbulent when the bubbles are indistinguishable. For the cases considered here churn-turbulent flow was observed at the air sparger tip near the bottom of the column for water, but most of the bubble formation occurred in the Stoke's and Taylor bubble regimes.

Water Test Results. Tests were performed at three different levels (4.3 feet, 11.9 feet, and 24.3 feet) and three different fill superficial velocities at each fluid level (2, 5,and 10 millimeter/second or 2.1, 5.2, and 10.5 scfm). Results at the 24.3 foot level are similar to results at other fluid levels. Accordingly results at this level are the discussion focus. Photos were taken through the viewports, which are identified in Fig. 4 as bottom, and second viewport from the bottom through fourth viewport from the bottom. Figure 8 dimensions one photograph taken through a typical viewport to provide orientation to the subsequent photos. To provide this orientation, the sparger tube and two opposing viewports are dimensioned. Multiple photos from individual viewports are shown as required in this paper, as

selected from numerous videos and hundreds of photos (Guerrero, et. al. [1]).

At the sparger tip, the flow is typically churn-turbulent, as shown in Figs. 8 and 9. Two of the available photos at the highest tested superficial velocity are shown to depict the unsteady nature of the flow at the sparger tip. Additional photos at lower velocities are shown in Figs. 10 and 11. The flow is still turbulent, but the bubbles are smaller as expected.

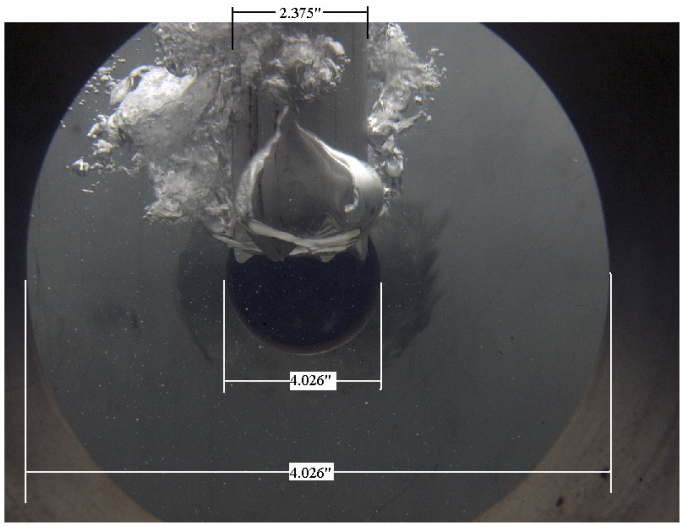

Figure 8: Bottom Viewport, 10.5 scfm, 24.3 Level

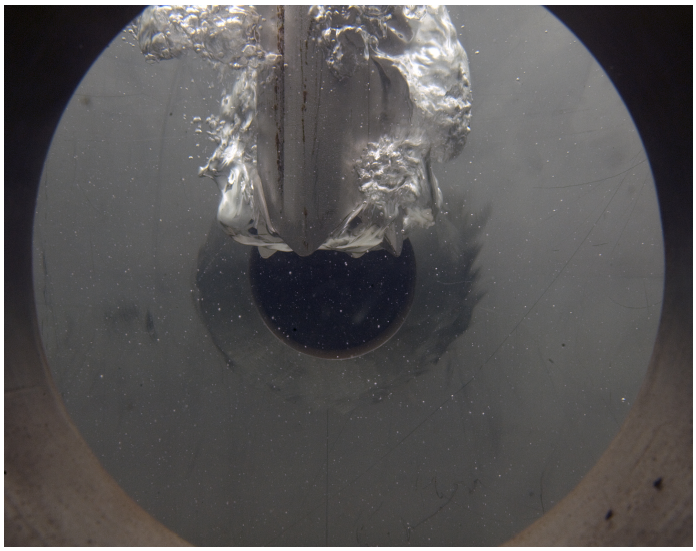

Figure 9: Bottom Viewport, 10.5 scfm, 24.3 Foot Level

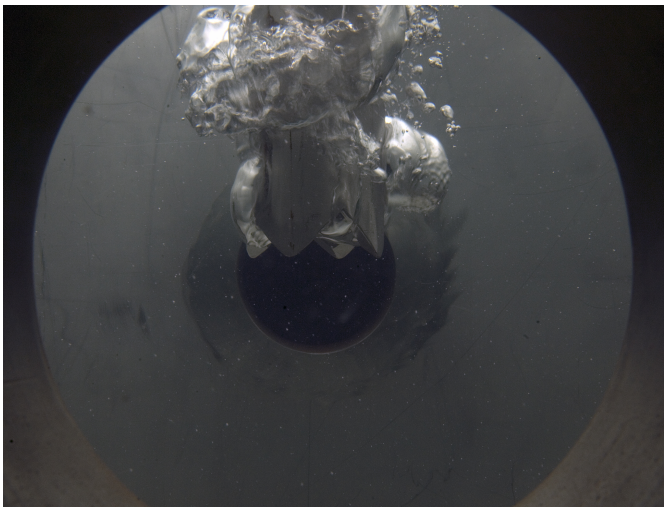

Figure 10: Bottom Viewport, 5.2 scfm, 24.3 Foot Level

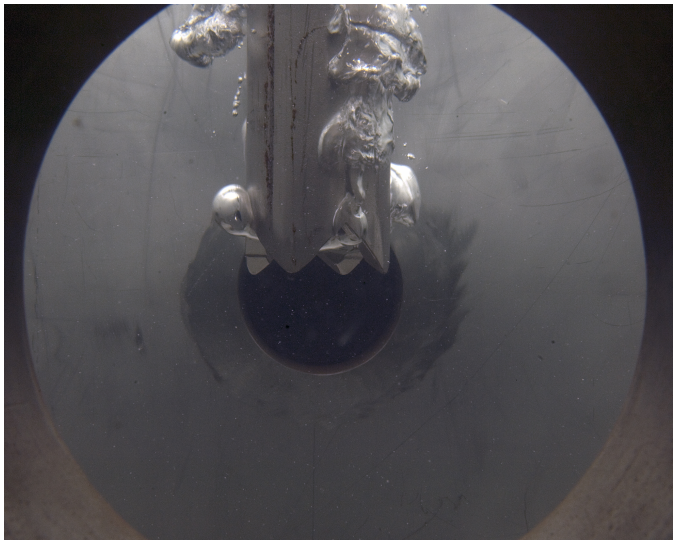

Figure 11: Bottom Viewport, 2.1 scfm, 24.3 Foot Level

As the bubbles rise from the sparger they form a cone of bubbles, which has an increasing diameter dependent on the flow rate. The flow is still rather unsteady, as shown in Figs. 12 and 13. The bubbles pass the viewport in swarms, rather than as a uniform flow of bubbles. For the 10.5 scfm flow, the bubble cone diameter is approximately 18 inches at the second viewport. At this viewport, the cone diameter is closer to a foot for the lowest 2.3 scfm flow. The change in bubble distribution due to flow rate is clearly seen by comparing Fig. 13 to Fig. 16.

The bubbles rise from the sparger to the surface in less than 30 seconds. As the bubbles rise, they form a more uniform pattern of bubbles as observed at the third and fourth viewports from the bottom (Figs. 16 - 22). Most of the bubbles travel upward through the center of the column, while some bubbles

travel downward along the column wall to recirculate the column contents.

Bubbles tend to enlarge as they exit the surface, and there is apparently little difference between bubble diameters at the surface for the velocities tested, as discerned from surface photos for the different velocities shown in Figs. 23 and 24.

Qualitatively, the uniformity of bubble distribution is largely dependent on flow rate and the vertical distance to the sparger tip. The higher the velocity and the further from the air supply, the more uniform the bubble distribution of 1/4 to 3/8 inch diameter bubbles.

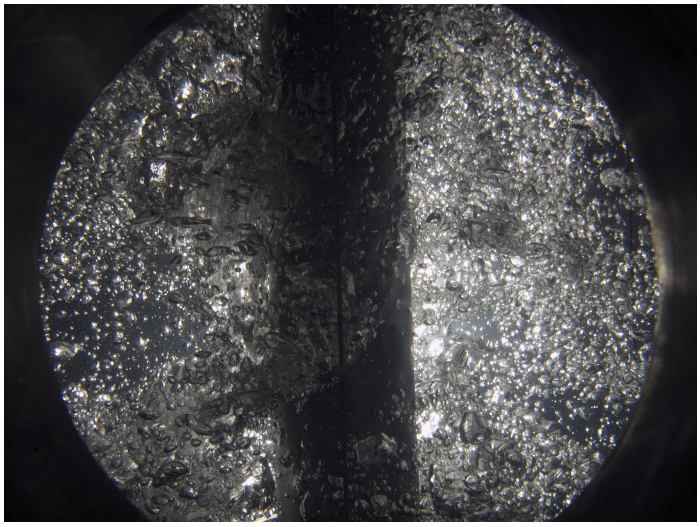

Figure 12: Second Viewport, 10.5 scfm, 24.3 Foot Level

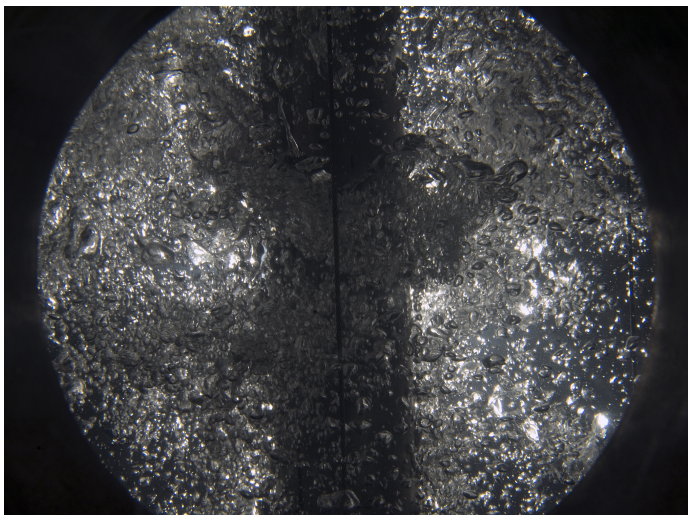

Figure 13: Second Viewport, 10.5 scfm, 24.3 Foot Level

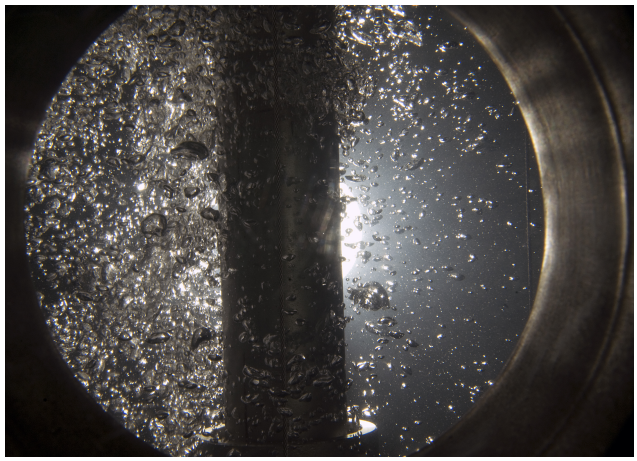

Figure 14: Second Viewport, 5.2 scfm, 24.3 Foot Level

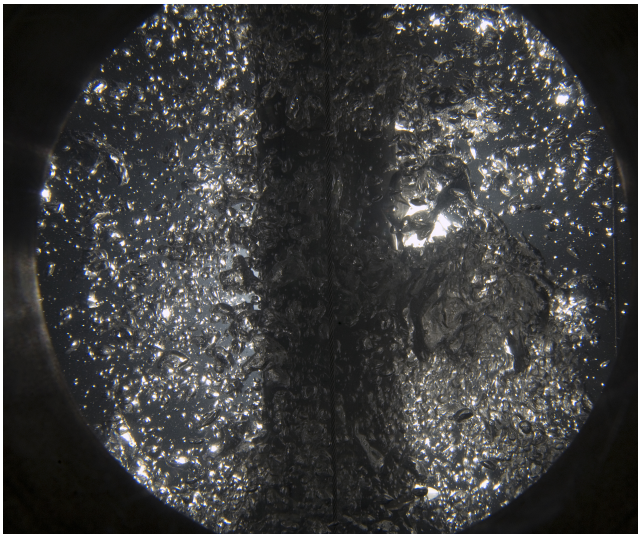

Figure 15: Second Viewport, 5.2 scfm, 24.3 Foot Level

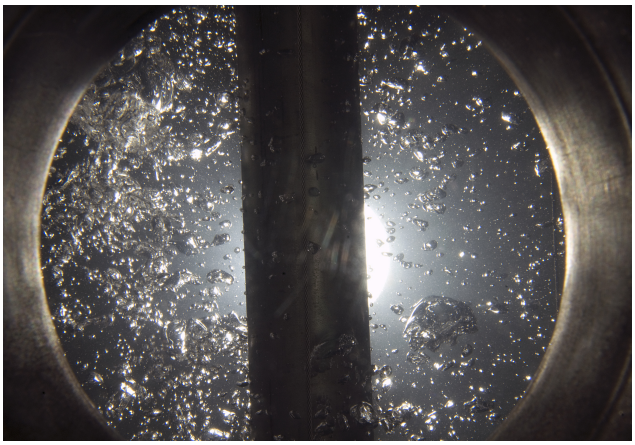

Figure 16: Second Viewport, 2.1 scfm, 24.3 Foot Level

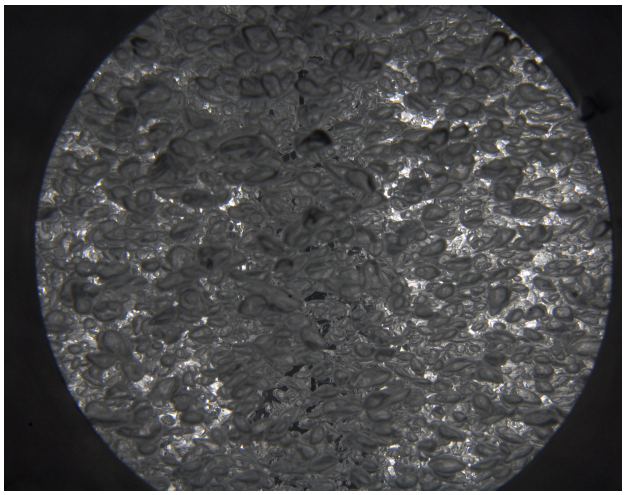

Figure 17: Third Viewport, 10.5 scfm, 24.3 Foot Level

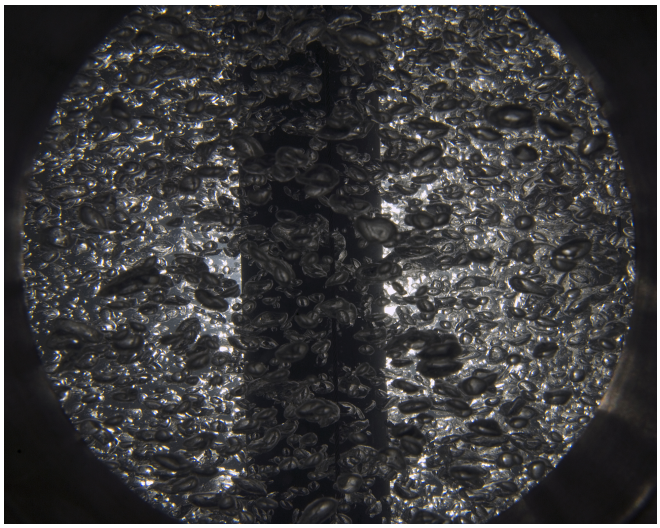

Figure 18: Third Viewport, 5.2 scfm, 24.3 Foot Level

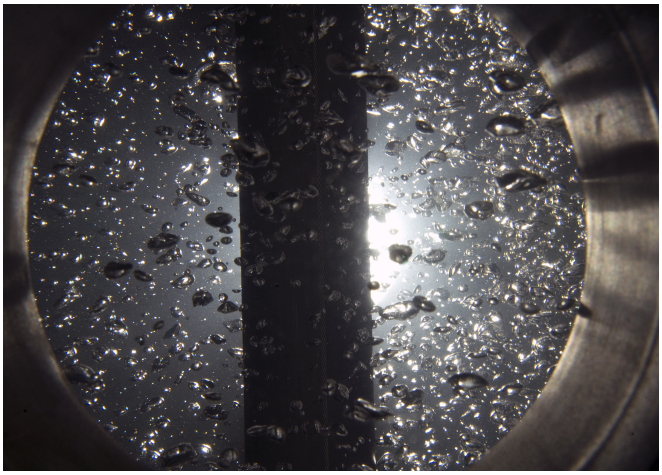

Figure 19: Third Viewport, 2.1 scfm, 24.3 Foot Level

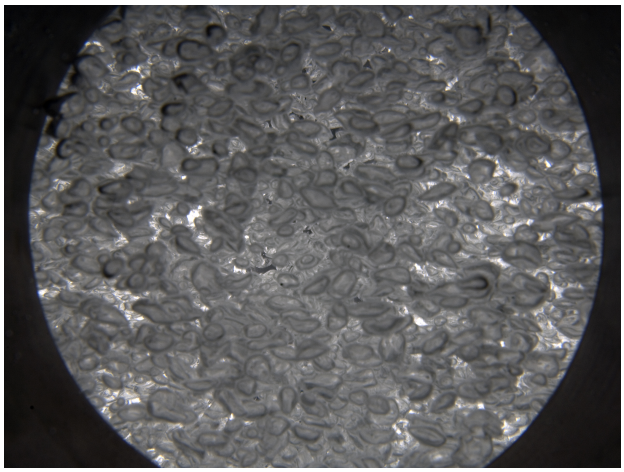

Figure 20: Fourth Viewport, 10.5 scfm, 24.3 Foot Level

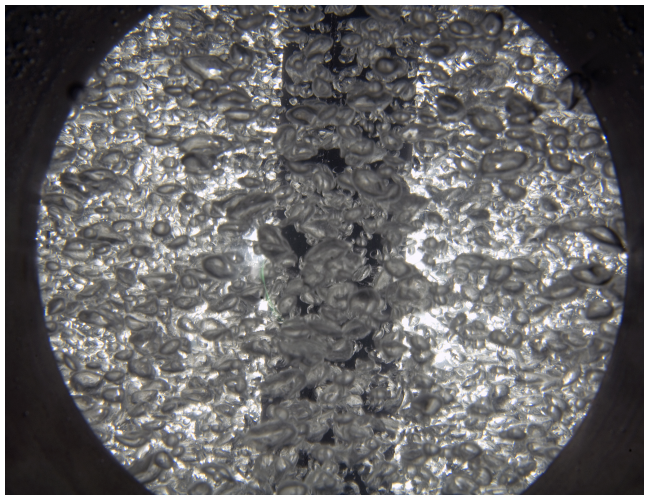

Figure 21: Fourth Viewport, 5.2 scfm, 24.3 Foot Level

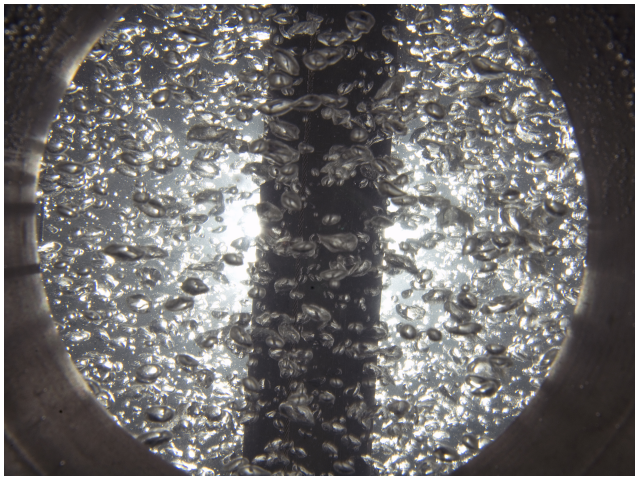

Figure 22: Fourth Viewport, 2.1 scfm, 24.3 Foot Level

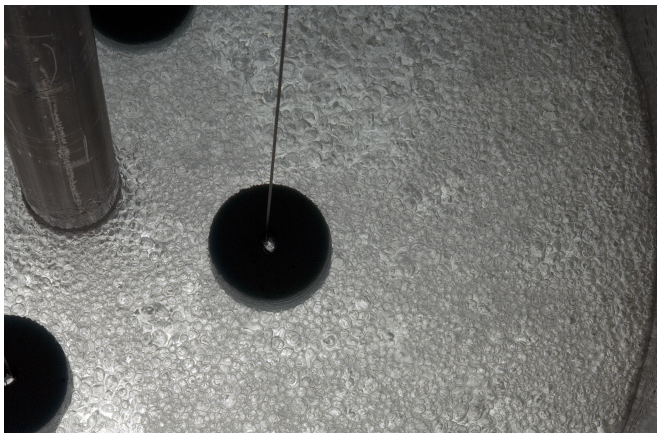

Figure 23: Surface, 5.2 scfm, 24.3 Foot Level

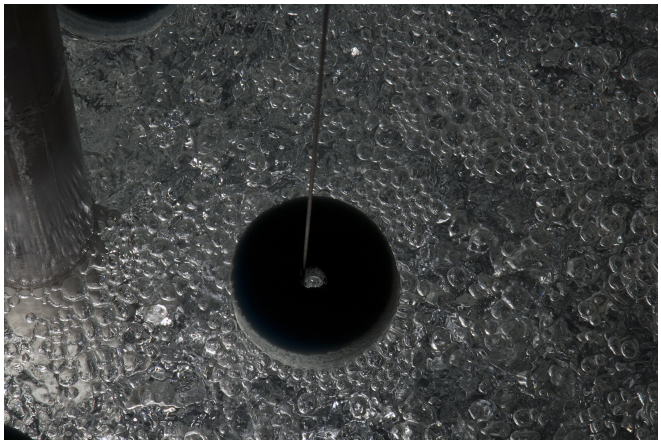

Figure 24: Surface, 2.1 scfm, 24.3 Foot Level

AZ101 Test Results. Tests using the AZ101 simulant provided significantly different results. Although photos could only be taken of the fluid surface, these show that large, single bubbles existed in the fluid. Instead of a distributed bubble field like that observed in water, large diameter bubbles exited the upper surface of the liquid. The maximum bubble diameters varied with flow rate between 2 and 8 inches for flows between 2.1 and 10.5 scfm. Although not shown in the photos, flow rates of 20 scfm created bubbles the size of the 30 inch diameter column.

Typical bubbles during testing of AZ101 are shown in Figs. 25 - 30. The stimulant was mixed thoroughly before testing. Figures 25 and 26 show successive video frames of bubble formations at the highest flow rates. Figures 28 and 29 can be compared to Fig. 25 to show an expected decrease in bubble size with decreased flow rate. As the flow rate decreases, the surface is agitated less violently by bursting bubbles, and less frequent but better defined bubbles occur, such as the one shown in Fig. 28. Figure 29 can be compared to Fig. 25 to observe that differences in bubble size were indiscernible for a higher yield stress material for the cases considered here. Figure 29 is the only figure for the 30 Pascal AZ101. Figure 30 can be compared to Fig. 25 to show that comparable bubble sizes were not significantly affected by the height of the fluid when it was varied from 4.3 to 24.3 feet.

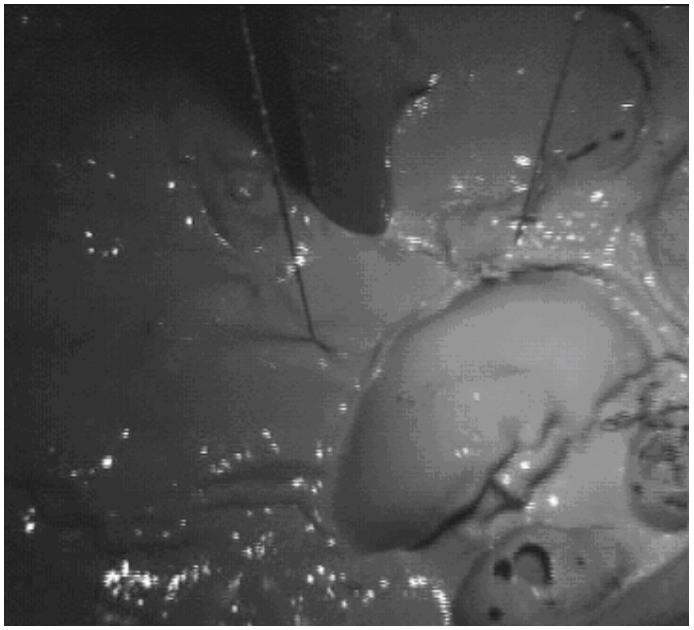

Figure 25: Surface, 10.5 scfm, 24.3 Foot Level

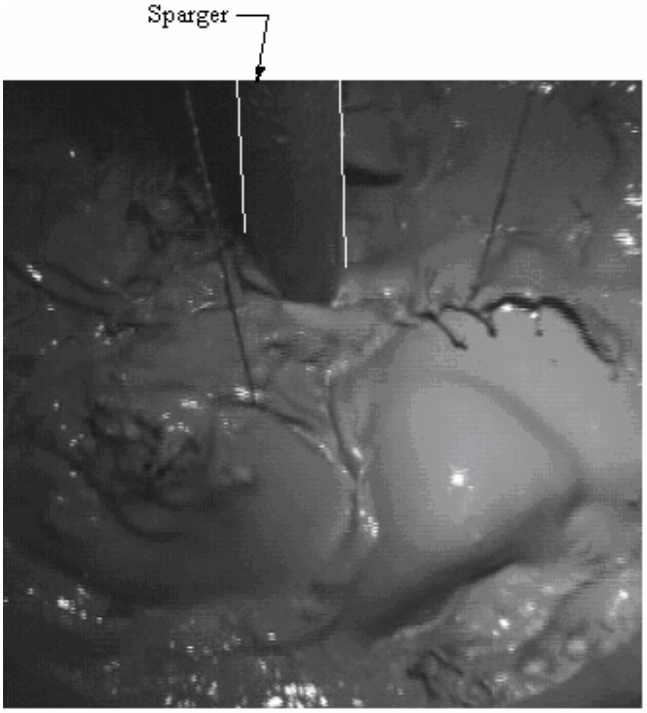

Figure 26: Surface, 10.5 scfm, 24.3 Foot Level, 72 milliseconds after Fig. 25

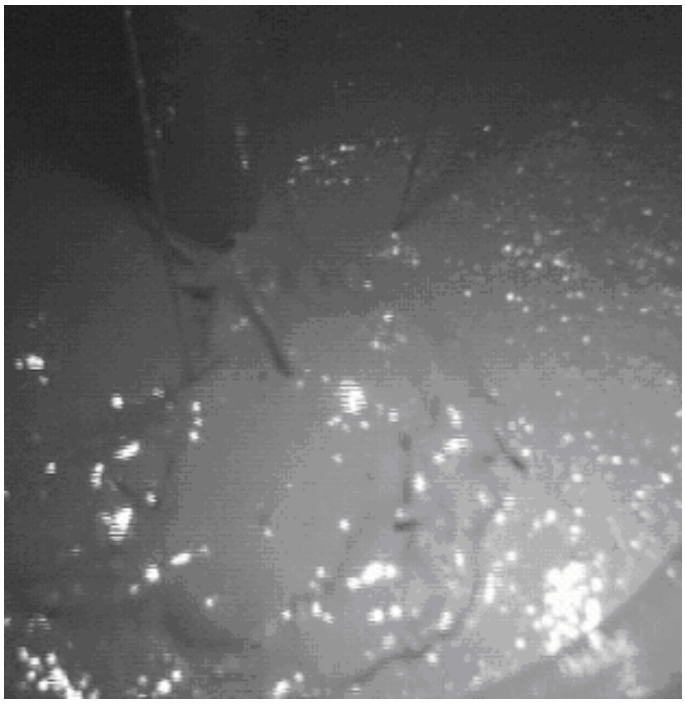

Figure 27: Surface, 5.2 scfm, 24.3 Foot Level

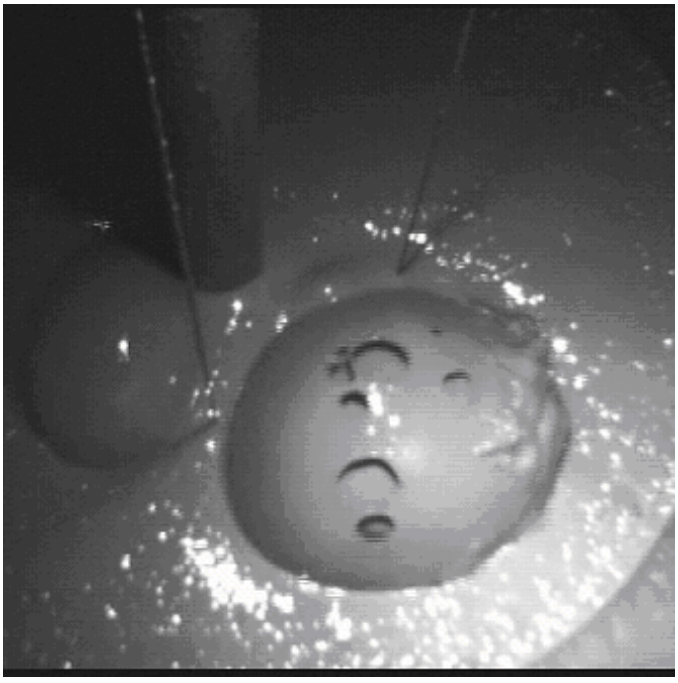

Figure 28: Surface, 2.1 scfm, 24.3 Foot Level

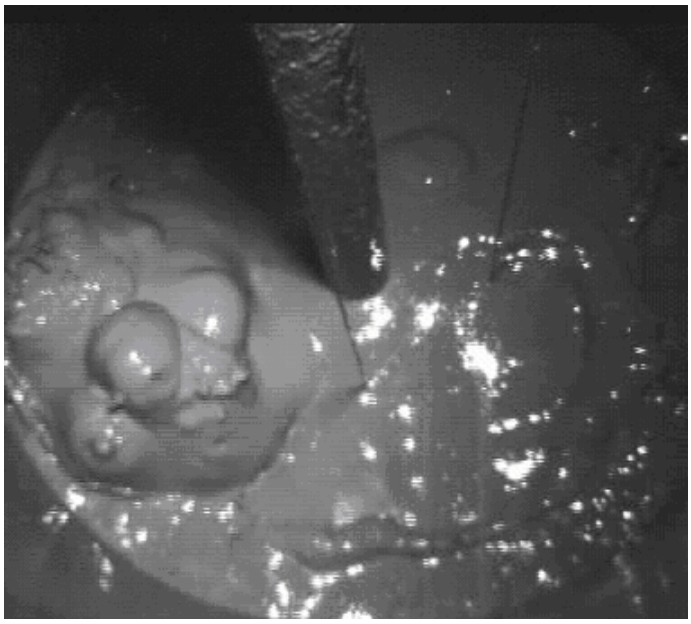

Figure 29: 30 pascal AZ101, Surface, 10.5 scfm, 24.3 Feet Level

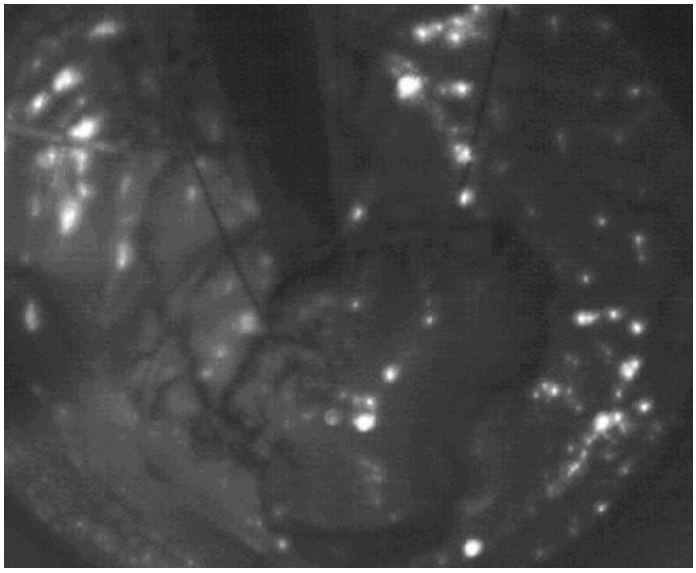

Figure 30: Surface, 10.5 scfm, 4.3 Foot Level

Laponite Test Results. The Laponite test results provided further insight into the complexities of bubble formation in Bingham plastic fluids (Restivo, et. al. [2], Larson [5], Gauglitz, et al. [6 and 7]). Laponite tests were performed in the column by varying the pressure and air flow to the sparger as shown in Figs. 6 and 7. An initial pressure was required to overcome the static head of the fluid at the sparger tip. Once this pressure was overcome, the fluid cracked, and formed fracture planes along which bubbles moved. The bubbles were even observed to jump from one crack to another. Effectively, the fluid acted elastically

at first, and then plastically at the yield stress, where it cracked in a manner similar to the cracking of a solid. As the pressure was increased, discrete bubbles were formed which rose to the surface. The Laponite has a higher yield stress than the Az101, and similar to the AZ101 simulant discrete bubbles were formed instead of a field of bubbles. Figures 31 - 36 further describe this behavior and require some discussion.

The Laponite was sheared by mixing and allowed to settle in the column for 24 hours before testing. Air pressure was increased to the column as shown in Fig. 31. Air flowed into the sparger tube and displaced the air in the tube until air flow started through the Laponite. The point at which air flow passed through the Laponite is noted as the breakthrough point on the figure. When breakthrough occurred, fracture paths were observed as shown in Fig. 32, and bubbles were observed to jump from one fracture to the next as the air moved upward. As the flow increased the bubble size increased. Bubble sizes of 1, 2 and 8 inch diameters were observed at 1, 2 and 6.5 scfm flow rates, and the bubbles are shown in Figs. 33 – 35. Similar to the recirculation noted in the water tests, Fig. 36 shows the approximate recirculation path noted during test.

Effectively, bubbles were created at the sparger tip, and they did not break up into smaller bubbles. This is the most significant difference between bubbles created in a Bingham fluid when compared to a Newtonian fluid. However, the yield stress and consistency required to separate the two types of behavior was indeterminate, due to the limited amount of data.

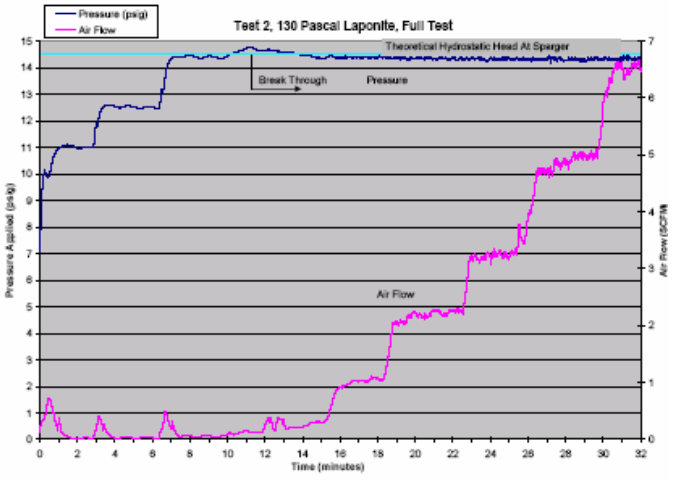

Figure 31: Air Addition During Laponite Testing

Figure 32: Fracture Paths created When Breakthrough of Air through the Laponite Occurred

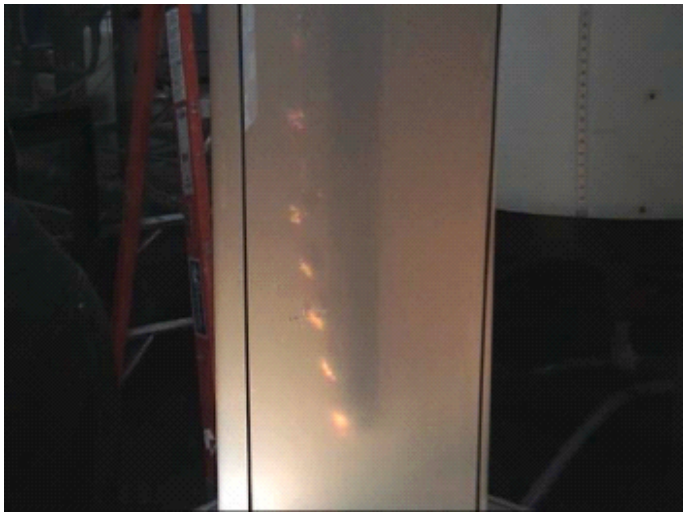

Figure 33: Bubbles in Laponite at 1 scfm

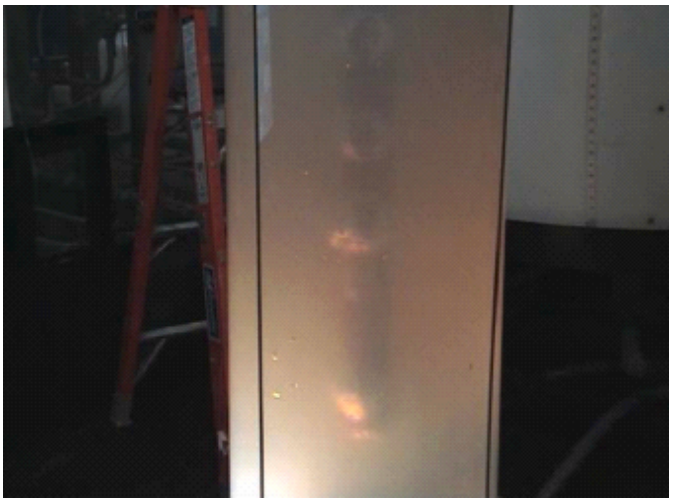

Figure 34: Bubbles in Laponite at 2 scfm

Figure 35: Bubbles in Laponite at 6.5 scfm

CONCLUSION

The behavior of Bingham plastic fluids is decidedly different than the behavior of Newtonian fluids with respect to bubble formation in large scale systems. When air was introduced to the bottom of an open tank, or column, the air bubbles broke up into many smaller bubbles in the Newtonian fluid. These bubbles rose to the surface of the column, forming a cone of bubbles from the sparger which then formed a continuous, uniform, field of bubbles as they rose. Qualitatively, the height at which a uniform field of bubbles formed was related to the air flow rate. The non-uniform cone of bubbles extended further up the column for lower air flow rates. In the non-Newtonian Bingham plastic fluids, the bubbles remained intact after they exited the sparger and rose to the surface. In other words, identical air flow conditions created significantly different bubble sizes dependent on fluid type. For Newtonian fluids, bubble sizes were observed to be1/4 to 3/8 inch in diameter for superficial velocities of 2 - 10 millimeters / second. For the non-Newtonian fluids at the same flow rates, the bubbles were observed to be 2 – 8 inches in diameter, when air flow rate was varied between superficial velocities of 2 and 10 mm/second. As the flow was increased even further, the bubble diameter equaled the 30 inch column diameter. In other words, Bingham fluids support significantly larger bubble formation than Newtonian fluids.

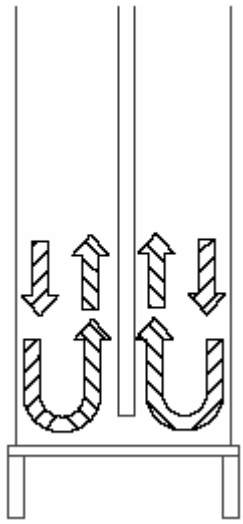

Figure 36: Recirculation Path of Fluid Due to Bubble Formation

REFERENCES

[1] H. N. Guerrero, C. L. Crawford, M. D. Fowley, R. A. Leishear, M. L. Restivo, "Effects of Alternate Antifoam Agents, Noble Metals, Mixing Systems, and Mass Transfer on Gas Holdup and Release from Non-Newtonioan Slurries", WSRC-TR-2007-00537.

[2] Restivo, M., Guerrero, H., "Final Report – UFP Restart and Sparger Testing", WSRC-TR-2004-00488.

[3] Clift, R., Grace, J. R., Weber, M. E., "Bubbles, Drops and Particles", 1978, Academic Press, Inc. Boston.

[4] Shaikh, A., and M.H. Al-Dahhan (2007). "A Review of Flow Regime Transition in Bubble Columns," *Int. J. Chem. Reactor Eng.*, **5**, R1.

[5] Larson, R.G. (1999). *The Structure and Rheology of Complex Fluids*, Oxford University Press, New York, NY.

[6] Gauglitz, P.A., and G. Terrones (2002). *Estimated Maximum Gas Retention from Uniformly Dispersed Bubbles in K Basin Sludge Stored in Large Diameter Containers*, PNNL-13893, Pacific Northwest National Laboratory, Richland WA, 99352.

[7] P.A. Gauglitz, G. Terrones, S.J. Muller, M.M. Denn, and W.R. Rossen (2002). *Final Report: Mechanics of Bubbles in Sludges and Slurries*, PNNL-13748, Pacific Northwest National Laboratory, Richland WA, 99352.